

## Spontaneous Optical Fractal Pattern Formation

J. G. Huang and G. S. McDonald

*Joule Physics Laboratory, School of Computing, Science and Engineering, Institute for Materials Research, University of Salford, Salford M5 4WT, United Kingdom*

(Received 21 January 2005; published 2 May 2005)

We report, for the first time, spontaneous nonlinear optical spatial fractals. The proposed generic mechanism employs intrinsic nonlinear dynamics both to generate an initial pattern seed and to fill out structure across decades of spatial scale. We demonstrate this in one of the simplest of nonlinear optical systems, composed of a Kerr slice and a single-feedback mirror. In this case, the smallest pattern scales are limited by either the optical wavelength or the diffusion length of the medium photoexcitation. The dimension characteristics of these particular fractals are also derived.

DOI: 10.1103/PhysRevLett.94.174101

PACS numbers: 05.45.Df, 42.65.Hw, 42.65.Sf

Complexity focuses on commonality across subject areas and forms a natural platform for multidisciplinary activities. Typical generic signatures of complexity include: (1) spontaneous occurrence of simple pattern (e.g., stripes, hexagons) emerging as a dominant nonlinear mode and (2) the formation of a highly complex pattern in the form of a fractal (with structure spanning decades of scale). However, to our knowledge, the following firm connection between these two signatures has not previously been established. This is perhaps not surprising since system nonlinearity tends to impose a specific scale, while fractals are defined by their scaleless character. Here we report a generic mechanism for spontaneous fractal spatial pattern formation; this mechanism has independence with respect to both the particular form of nonlinearity and the particular context of the nonlinear system.

In the photonics domain, Berry [1] established that fractal light may be generated in simple *linear* optical systems. More recently, the highly-structured (linear) modes of unstable-cavity lasers were discovered to be fractal in character [2], and optical fractal generators based upon introducing electronic feedback or nonlinearity have also been developed [3].

In this Letter, we propose intrinsic *nonlinear* dynamics providing *both* the necessary feedback mechanism and the pattern seed for building fractals. We demonstrate this generic mechanism by considering one of the simplest optical pattern-forming systems.

The system, shown in Fig. 1, is composed of a thin slice of Kerr medium, illuminated from one side by a spatially smooth beam, and a feedback mirror (with reflectivity  $R$ ) a distance  $d$  away (note: all variables are dimensionless) [4]. The photoexcitation density  $n$  in the medium has a relaxation time  $\tau$  and a diffusion length  $l_D$ . The thickness  $L$  of the Kerr medium is sufficiently small that diffraction of light over this distance can be neglected. The evolution of fields over distance  $z$  and the development of  $n$ , in time  $t$ , is then described by

$$\frac{\partial F}{\partial z} = i\chi n F \quad (1a)$$

$$\frac{\partial B}{\partial z} = -i\chi n B \quad (1b)$$

$$-l_D^2 \nabla_{\perp}^2 n + \tau \frac{\partial n}{\partial t} + n = |F|^2 + |B|^2, \quad (1c)$$

where  $\chi$  parametrizes the Kerr effect (positive for self-focusing, negative for self-defocusing),  $\nabla_{\perp}^2$  is the transverse Laplacian, and  $F$  and  $B$  are the transverse profiles of the forward and backward fields, respectively. The Fourier transforms of these profiles,  $F(K, t - T_R)$  and  $B(K, t)$ , are related through

$$B(K, t) = \sqrt{R} \exp(-i\theta) F(K, t - T_R) \quad (2a)$$

$$\theta = \left(\frac{2d}{k_0}\right) \frac{K^2}{1 + \sqrt{(1 - K^2/k_0^2)}}, \quad (2b)$$

where  $k_0$  is the free space wave number and  $T_R$  is the cavity transit time. Note that in Eq. (2a) there is a time delay between  $B(K)$  and  $F(K)$ , arising from diffractive propagation. Equations (1) and (2) thus constitute a delay-differential system.

Linear stability analysis [4] yields a threshold condition for growth of spontaneous spatial pattern:

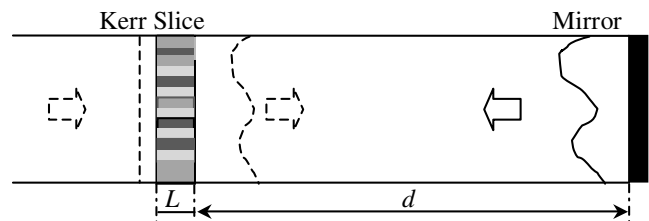


FIG. 1. Schematic diagram of the Kerr slice with single-feedback mirror system. Spatial fluctuations in the carrier density modulate the phase of the field (dashed line) and diffraction changes this into an amplitude modulation (solid line).

$$|\chi|I_{th}L = \frac{1 + K^2 l_D^2}{2R|\sin(K^2 d/k_0)|}, \quad (3)$$

when  $K^2 \ll k_0^2$  and where, for a focusing medium ( $\chi > 0$ ),

$$\sin(K^2 d/k_0) > 0. \quad (4)$$

Figure 2(a) shows that the curves for threshold intensity  $I_{th}$  actually divide frequency space into an infinite number of bands, whose widths and separations decrease with increasing  $K$ . The minimum thresholds of the bands generally increase smoothly with increasing  $K$ .

If one assumed independent growth of Fourier modes, then one could estimate the transverse power spectrum to be proportional to  $I_0 - I_{th}$ , when  $I_0 > I_{th}$ , for incident plane-wave intensity  $I_0$ . The power spectrum would then have a shape similar to that shown in Fig. 2(b). Comparing this spectrum with known spectra of fractal laser modes [5], we note that both are composed of *discrete* frequency bands. In fractal laser modes, a fine detail (diffraction) pattern seed has larger scale patterns superimposed and this defines a power spectrum that gives a (generally) scale-dependent fractal dimension [5]. Here, an initial spontaneous pattern seed is expected to form at the largest scale, whereby nonlinear processes may also generate patterns at successively smaller scales. Thus, it is plausible that fractal pattern formation could result here and, in fact, in *any* nonlinear system that has characteristics similar to those in Fig. 2.

For simplicity, we first consider a local Kerr effect ( $l_D = 0$ ) and an effectively instantaneous response ( $\tau = 0$ ). The resulting threshold characteristic [Fig. 2(c)] exhibits minimum thresholds, from each frequency band, that are equal. If the incident plane-wave intensity is slightly higher than this (global) minimum  $I_{min}$ , spatial frequencies defined by the minima of the bands will all have the same growth rate. One then expects the resultant intensity distribution across the two (transverse) dimensional plane to be an extremely complicated (volume-filling) pattern with fractal dimension 3.

To permit visualization and verification of results for this configuration, we propose introduction of spatial filtering in the free space path, whereby bandwidth-limiting control can be freely adjusted. Patterns generated for a range of control setting can be illustrated in the dynamic evolution

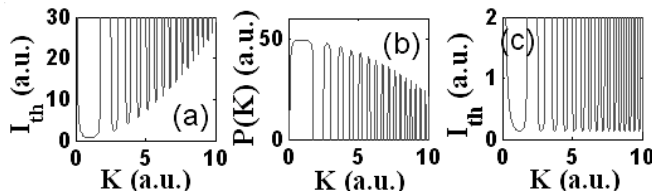


FIG. 2. (a) Instability threshold and (b) qualitative sketch of power spectrum ( $I_0 = 50$ ) for the Kerr slice with single-feedback mirror system ( $l_D = 1$ ,  $d/k_0 = 1$ ,  $R = 0.9$ ,  $\chi L = 1$ ,  $K^2 \ll k_0^2$ ). (c) as (a), but  $l_D = 0$ .

of a single simulation of the model equations. Within the framework of the current model, we introduce a filtering function  $f(K; k_c) = \theta(K; k_0)$  so that components with  $K > k_c$  are attenuated. Conventional (single- $K$ ) pattern formation [6] is demonstrated by setting  $k_c$  so that only frequencies in the first instability band propagate freely.

For a given plane-wave input field, we initiate the photo-excitation density with the corresponding steady-state profile and add a small (1%) level of white noise. After  $100 T_R$ , the transverse profile of the backward field intensity becomes the static hexagonal pattern shown in Fig. 3(a). We then instantaneously remove the filter ( $k_c \rightarrow \infty$ ) and monitor the subsequent evolution. Three of the resulting patterns are shown in Figs. 3(b)–3(d). Evolution is from simple hexagon to patterns with increasing level of details. This evolution continues with development of details as small as the scale of the optical wavelength.

We also simulate the system with just one transverse dimension ( $x$ ). Pattern and power spectrum evolution in the backward field intensity, from a simple pattern to a fractal one, is shown for this case in Fig. 4. Figure 4(a) shows the pattern formed under the same conditions as in Fig. 3(a). Its power spectrum shows that this pattern is composed of a single frequency plus harmonic contributions [6]. After the filter is removed, the spatial patterns become progressively more complicated. Sets of harmonic frequencies, associated with each instability band, grow very rapidly and lead the growth of the high frequency edge of the power spectra. After  $150 T_R$ , all frequency components plotted have reached an intensity of the same order of magnitude. The system then continues to evolve, but the statistical distri-

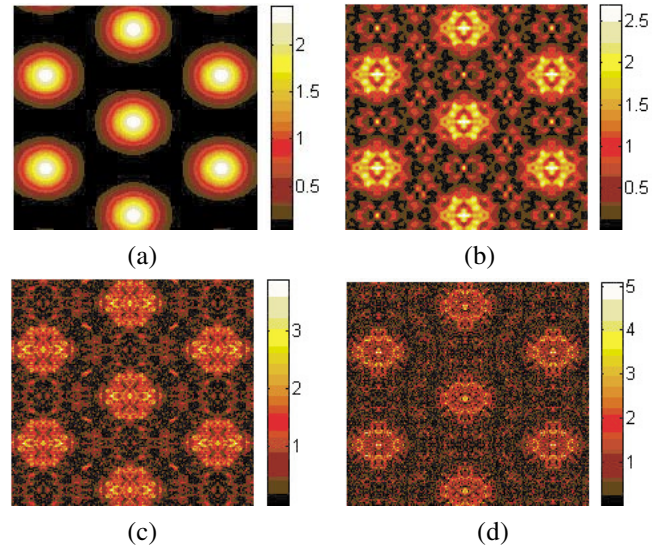


FIG. 3 (color online). Transverse pattern evolution of the system for  $l_D = 0$ ,  $\tau = 0$ ,  $d/k_0 = 1$ ,  $\chi L = 1$ ,  $I_0/I_{min} = 2$ , and  $R = 0.9$ . (a) Hexagonal pattern formed by introducing a one-band-pass frequency filter ( $t = 100T_R$ ,  $k_c = 2$ ). (b), (c), and (d) are patterns after the filter is removed: (b)  $t = 103T_R$ , (c)  $t = 106T_R$ , (d)  $t = 109T_R$ .

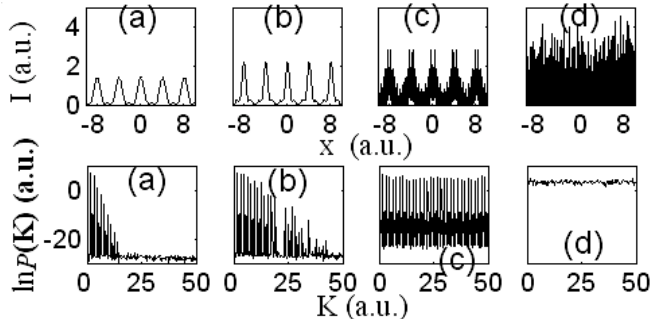


FIG. 4. Spatial pattern evolution in time (upper row) and the corresponding power spectra (lower row):  $l_D = 0$ ,  $\tau = 0$ ,  $d/k_0 = 1$ ,  $\chi L = 1$ ,  $I_0/I_{\min} = 2$ , and  $R = 0.9$ . (a) With a one-band-pass frequency filter ( $t = 100T_R$ ,  $k_c = 2$ ). (b), (c), and (d) are patterns after the filter is removed. (b)  $t = 102T_R$ , (c)  $t = 113T_R$ , (d)  $t = 150T_R$ .

bution of power across the frequencies remains invariant. Thus, subsequent patterns have the same fractal dimension of 2.

One could consider the fractal patterns of this system as constructed with an infinite number of simple patterns of different sizes, as in [7]. But here, both the initiation and prefractal generation stages arise from nonlinear optical processes. The fractal formation process is thus quite distinct from simple multiplication or summation of different-size patterns, such as in image processing or in unstable-cavity lasers [5].

Figure 5 shows dynamic evolution of the optical power spectrum when medium diffusion is included ( $l_D \neq 0$ ) and no spatial filtering is employed. The rate of bandwidth growth does depend on system parameters, such as the intensity of the incident field, but fractal formation is nonetheless very fast (typically less than  $50 T_R$ ). After that time, the system enters a dynamic equilibrium state in which the average power spectrum remains unchanged, even though the pattern in real space continues to evolve. Figures 5(c) and 5(d) demonstrate this statistical invariance in frequency space and that an appreciable portion of the dynamic state is well described by a linear relationship.

Figure 6 highlights how this linear relationship changes with the value of diffusion length. For each set of parameters, linear regression has been used to quantify the dynamic equilibrium state and a summary of these

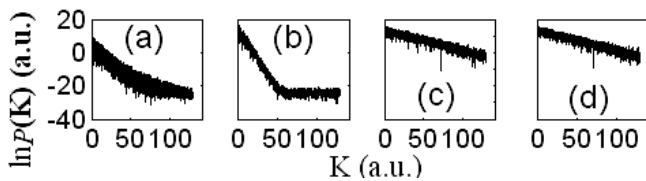


FIG. 5. Power spectrum evolution in time: (a)  $t = 2T_R$ , (b)  $t = 5T_R$ , (c)  $t = 50T_R$ , (d)  $t = 2000T_R$  ( $l_D = 0.1$ ,  $d/k_0 = 100$ ,  $\tau = 1$ ,  $R = 0.9$ ,  $\chi L = 1$ ,  $I_0 = 3.0$ ).

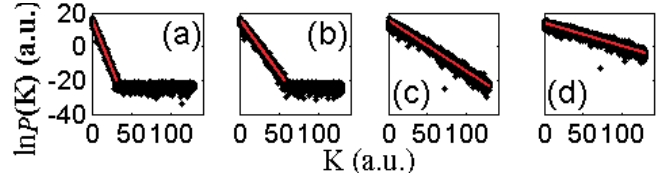


FIG. 6 (color online). Variation of equilibrium power spectra with diffusion length  $l_D$ : (a)  $l_D = 0.8$ , (b)  $l_D = 0.4$ , (c)  $l_D = 0.2$ , (d)  $l_D = 0.1$  ( $d/k_0 = 100$ ,  $\tau = 1$ ,  $R = 0.9$ ,  $\chi L = 1$ ,  $I_0 = 3.0$ ,  $t = 1500T_R$ ).

characteristics is presented in Fig. 7. The slope  $b$  is found to vary linearly with  $l_D$ . Figure 7(b) shows the relation between the slope and intensity of the input wave  $I_0$ ; the line fitted has equation  $b = b_1/I_0$ , where  $b_1$  denotes a constant. The experimental points agree with the fitted lines very well. These results support our claim that the dependence of the slope  $b$  on  $l_D$  and  $I_0$  is given by

$$b = b_0 l_D / I_0, \quad (5)$$

where  $b_0$  is a constant dictated by system parameters.

The average trend of each equilibrium power spectrum can be represented as

$$\ln P(K) = a + bK, \quad (6)$$

where  $a$  and  $b$  are constants dictated by system parameters. Using [5]

$$D = \frac{1}{2} \left[ 5 + \frac{d(\ln P)}{d(\ln K)} \right], \quad (7)$$

an expression for the power spectrum fractal dimension is obtained:

$$D(K) = \frac{5}{2} + \frac{b}{2} K. \quad (8)$$

For the above calculations using one transverse dimension,  $D$  must be between 1 and 2. So the equation for the fractal

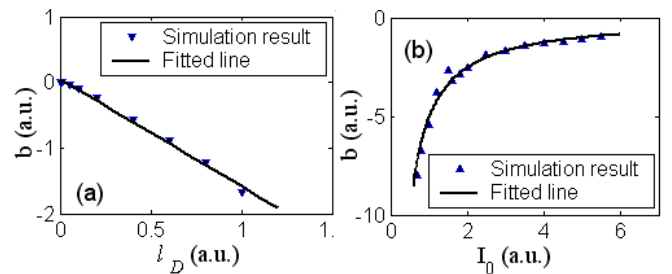


FIG. 7 (color online). Variation of the slope  $b$  of the equilibrium power spectrum vs (a) diffusion length  $l_D$  and (b) intensity of the incident plane wave  $I_0$ . Parameters are  $d/k_0 = 100$ ,  $\tau = 1$ ,  $R = 0.9$ ,  $\chi L = 1$ . (a) has  $I_0 = 3.0$ ; (b) has  $l_D = 0.1$ .

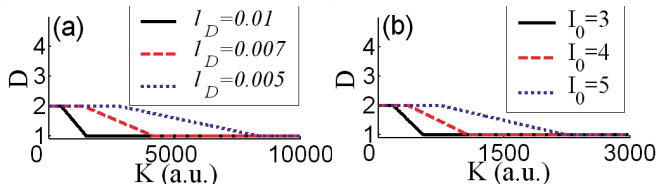


FIG. 8 (color online). Variation of fractal dimension vs space frequency  $K$  for different values of: (a) diffusion length  $l_D$  when  $I_0 = 3.0$ ; (b) intensity of the incident wave  $I_0$  when  $l_D = 0.01$  ( $d/k_0 = 100$ ,  $R = 0.9$ ,  $\chi L = 1$ ).

dimension should be written as

$$D(K) = \begin{cases} 2 & K < -1/b \\ \frac{5}{2} + \frac{b}{2}K, & \text{when } -1/b \leq K \leq -3/b. \\ 1 & K > -3/b \end{cases} \quad (9)$$

Figure 8 shows the variation of this fractal dimension with spatial frequency  $K$  as a function of diffusion length  $l_D$  and intensity of the incident wave  $I_0$ . Each pattern has a fractal dimension of 2 within the low frequency regime and this value changes linearly to 1 in the midfrequency range. In the high frequency section, each pattern has a dimension of 1. We thus classify the patterns generated by this system as *scale-dependent fractals* [5]. We note that both the low frequency range and the midfrequency range increase in size with either a decrease in  $l_D$  or an increase in  $I_0$ , and that  $K < -1/b$  for all  $K$  when  $l_D \rightarrow 0$ .

To verify our results, we have also used the software package BENOIT 1.3 [8] to calculate the variogram dimension of the output patterns:

$$D_v = 2 - \frac{1}{2} \frac{d(\ln V)}{d(\ln W)}, \quad (10)$$

where the variogram  $V$  is defined as the expected value of the squared difference of intensities at two points separated by distance  $W$  (the window interval length).

Considering typical patterns, the log-log plot of  $V$  versus  $W$  (Fig. 9) has a tangent gradient  $S$  that decreases smoothly from 2 to 0 when  $W$  increases from small scales ( $W = 1$  in Fig. 9) to larger scales ( $W = 100$  in Fig. 9). The average slope remains 0 when  $W > 100$ . From the definition  $D_v = 2 - S/2$ , this fractal dimension increases from 1 to 2 when  $W$  increases from 1 to 100, and  $D_v = 2$  for larger  $W$ . The fractal dimension of the pattern is thus found to decrease smoothly from 2 to 1 with increase in spatial frequency. These results are consistent with those found by using the power spectrum method, and hence substantiate our claims regarding the fractal dimension of the patterns generated. When two transverse dimensions are considered, the above fractal dimensions each increase by 1.

In conclusion, the first prediction of spontaneous fractal pattern formation in an all-optical nonlinear system has

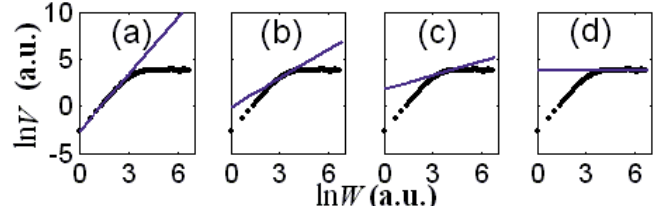


FIG. 9 (color online). Variogram of the intensity of the backward field vs window interval length  $W$  ( $I_0 = 3.0$ ,  $l_D = 1$ ,  $d/k_0 = 100$ ,  $\tau = 1$ ,  $R = 0.9$ ,  $\chi L = 1$ ). (a)  $W = 1$ ,  $S = 1.996$ ,  $D_v = 1.002$ ; (b)  $W = 27$ ,  $S = 1.002$ ,  $D_v = 1.499$ ; (c)  $W = 46$ ,  $S = 0.49$ ,  $D_v = 1.755$ ; (d)  $W = 100$ ,  $S = 0$ ,  $D_v = 2$ .

been presented. We believe that this is a generic mechanism that can arise in a wide variety of nonlinear systems. The particularly simple system studied here generates optical fractals whose smallest scale is limited by either: (a) the optical wavelength or (b) diffusion of the medium photoexcitation. Inclusion of a spatial filter has allowed us to demonstrate both conventional (single frequency) pattern formation and fractal formation in the same system. In the diffusion-limited system, we discovered that the dependence of spectral characteristics on the carrier diffusion length and the input pump intensity is given by a rather simple law. An analytical form was thus derived for this (scale-dependent) fractal dimension, and predictions were confirmed by variogram analysis.

This work is supported by Overseas Research Studentship Grant No. 2002035004 and the University of Salford.

- [1] M. V. Berry, I. Marzoli, and W. Schleich, *Phys. World* **14** (6), 39 (2001), and references therein.
- [2] G. P. Karman and J. P. Woerdman, *Opt. Lett.* **23**, 1909 (1998); G. P. Karman, G. S. McDonald, G. H. C. New, and J. P. Woerdman, *Nature (London)* **402**, 138 (1999); G. S. McDonald, G. P. Karman, and G. H. C. New, *J. Opt. Soc. Am. B* **17**, 524 (2000).
- [3] J. Courtial, J. Leach, and M. J. Padgett, *Nature (London)* **414**, 864 (2001).
- [4] W. J. Firth, *J. Mod. Opt.* **37**, 151 (1990).
- [5] G. H. C. New, M. A. Yates, J. P. Woerdman, and G. S. McDonald, *Opt. Commun.* **193**, 261 (2001); M. V. Berry, C. Storm, and W. V. Saarloos, *Opt. Commun.* **197**, 393 (2001).
- [6] G. D'Alessandro and W. J. Firth, *Phys. Rev. Lett.* **66**, 2597 (1991).
- [7] W. H. Southwell, *Opt. Lett.* **6**, 487 (1981); W. H. Southwell, *J. Opt. Soc. Am. A* **3**, 1885 (1986); J. Courtial and M. J. Padgett, *Phys. Rev. Lett.* **85**, 5320 (2000).
- [8] BENOIT 1.3, TruSoft International, Inc., <http://www.trusoft.netmegs.com/benoit.html>.